

# Electroweak phase transition with the confinement scale of the strong sector or Dilaton in the minimal composite Higgs model

Vo Quoc Phong<sup>a,b\*</sup> and Truong Van Tien<sup>a,b†</sup>

<sup>a</sup>*Department of Theoretical Physics, University of Science, Ho Chi Minh City 70000, Vietnam*

<sup>b</sup>*Vietnam National University, Ho Chi Minh City 70000, Vietnam*

Phan Hong Khiem<sup>c,d‡</sup>

<sup>c</sup>*Institute of Fundamental and Applied Sciences,*

*Duy Tan University, Ho Chi Minh City 700000, Vietnam*

<sup>d</sup>*Faculty of Natural Sciences, Duy Tan University, Da Nang City 50000, Vietnam*

The minimal Composite Higgs model (MCHM) provides an effective trigger for the Baryogenesis scenario through the confinement scale of the strong sector ( $f$ ) or Dilaton ( $\chi$ ).  $f$  is a parameter with mass dimension, which stores the resonances of particles at high energies, has a suitable value of about 800 GeV. But when  $300 \text{ GeV} \leq f \leq 400 \text{ GeV}$ , the effective Higgs potential has a first order electroweak phase transition. Therefore, although  $f$  cannot be a perfect trigger, it does suggest an effective approach that accommodates the resonances of particles. Thus the investigation of the electroweak phase transition according to  $f$  has confirmed that the inclusion of Dilaton in the effective potential is reasonable. Accordingly, we derive a Dilaton potential with appropriate parameter domains and  $f = 800 \text{ GeV}$ , the mass of Dilaton ranges from 300 GeV to 700 GeV, which will give an electroweak phase transition strength greater than 1 and less than 3, enough for a first order phase transition. This is a directly and clearly prove of the triggers for the first order EWPT in MCHM.

PACS numbers: 11.15.Ex, 12.60.Fr, 98.80.Cq

---

\* vqphong@hcmus.edu.vn

† tvtien832@gmail.com

‡ phanhongkiem@duytan.edu.vn

Keywords: Spontaneous breaking of gauge symmetries, Extensions of electroweak Higgs sector, Particle-theory models (Early Universe)

## CONTENTS

I. INTRODUCTION	2
II. Review on the minimal composite Higgs model	4
A. Spectra of particles	6
B. The effective Higgs potential	9
III. EWPT with the confinement scale of the strong sector	11
IV. EWPT with Dilaton	13
A. The Higgs-Dilaton potential in MCHM at 0K	14
B. The Dilaton potential	16
C. The potential at high temperature	17
D. The numerical results	19
V. CONCLUSION AND OUTLOOKS	23
ACKNOWLEDGMENTS	25
References	25

## I. INTRODUCTION

The baryogenesis scenario associated with Sakharov's conditions [1], is analyzed in a wide variety of models with different triggers [2–45]. Most of them are associated with a new physical prediction such as an energy scale, a dark matter candidate [2, 18, 46] or a change in some coupling in the SM [47, 48].

The Composite Higgs model [49] is also a possible solution to this problem. The model argues that SM is in fact an effective theory and the influence of very high energy physics on the current effective theory at low energies through the condensation of strongly bound states before the electroweak symmetry breaking occurs, and can spontaneously trigger the

EWPT. In addition to the EWPT, the model helps explain the origin of the Higgs particle which is actually formed from the symmetry breaking of a larger group at high energies.

However, there is no basis for determining the high-energy symmetry group, which is the core of a Composite Higgs Model. The Composite Higgs Model (CHM) borrows ideas from the Technicolor model to explain the origin of the Higgs particle as well as the complex doublet  $\phi$  that appears in the Standard Model Lagrangian. The CHM suggests that the complex bilinear is formed by Nambu Goldstone Bosons (NGBs) arising from the breaking of the symmetry group  $\mathcal{G}$  to the symmetry group  $\mathcal{H}$  such that the electroweak group  $\mathcal{G}_{EW} \subset \mathcal{H}$ , and the Higgs particle is a pseudo-NGB (pNGB) among these NGBs. The non-SM fields that appear at high energies will become effective interactions between elementary particles at low energies, and the SM is now an effective theory. Therefore, the Lagrangian of CHM now needs to be modified due to the influence of non-fundamental fields, also known as CFT fields. The part of the Lagrangian related to these fields is called the composite part. In the scope of this paper, we choose the minimal Composite Higgs model (MCHM) [53] to investigate, in which the Higgs doublet is parameterized in the  $SO(5)/SO(4)$  coset.

Therefore, many different Composite Higgs models have been studied, many of which are still insufficient to trigger electroweak symmetry breaking [50]. Besides the efforts to find a suitable symmetry group, it has been theorized that it is possible to modify the Composite Higgs model by "adding" the dilaton field [51, 52].

First of all we can make a general observation that in MCHM, the meson resonance components (stored in the confinement scale of the strong sector ( $f$ ) or the parameters of effective potential) and Dilaton will push the effective potential differently from SM and make the phase transition more violent than SM. This has been pointed out in Refs.[51, 52]. But with a large number of parameters, specifying a first order EWPT is quite difficult. Therefore, we will conduct the survey of the EWPT process using a method tentatively called like-SM in Sec.II.

The paper has the following structure. Except for the Introduction (Sec. I) and the Conclusion and Outlooks (Sec. V), the paper quantitatively demonstrates the EWPT process with a single-loop effective potential. Sec. II give a quick review of CHM, as well as comments and remarks on the masses of particles in CHM. In Sec. III, the effective potential will be studied; then, the EWPT strength will be calculated for different values of  $f$ . In Sec. IV, the effective Higgs-Dilaton potential is used to recalculate  $S$  for a mass range of Dilaton.

## II. REVIEW ON THE MINIMAL COMPOSITE HIGGS MODEL

Unlike the SM, where the Higgs doublet is initially unknown, in the CHM it is created by another symmetry breaking. Therefore, when studying the CHM, we need to specifically determine the vacuum state in order to specifically analyze the breaking of  $\mathcal{G} \rightarrow \mathcal{H}$  before the electroweak breaking occurs.

In general, the group  $\mathcal{G}$  has a Lie group algebra generated by generators  $T^A$ .  $T^A$  is divided into two parts: the unbroken generators  $T^a$  ( $a = 1 \dots \dim[\mathcal{H}]$ ) are the Lie algebraic basis of the group  $\mathcal{H}$ , and the broken generators  $\hat{T}^{\hat{a}}$  ( $\hat{a} = 1 \dots \dim[\mathcal{G}/\mathcal{H}]$ ). From this, a vacuum configuration of the composite part  $\vec{F}$  can be chosen such that

$$T^a \vec{F} = \vec{0}, \quad \hat{T}^{\hat{a}} \vec{F} \neq \vec{0}. \quad (1)$$

The NGBs  $\theta^{\hat{a}}$  are parameterized as a local transformation in the direction of  $\hat{T}^{\hat{a}}$  generators:

$$\vec{\Phi}(x) = \exp \left[ i \theta^{\hat{a}}(x) \hat{T}^{\hat{a}} \right] \vec{F}. \quad (2)$$

Then, if  $\theta$  reaches VEV  $\langle \theta \rangle \neq 0$ , it will cause the breaking of  $\mathcal{G}_{EW}$  symmetry in  $\mathcal{H}$ . Geometrically,  $\langle \theta \rangle$  is the angle between  $\vec{F}$  and  $\vec{\Phi}$ . The breaking of  $\mathcal{G}_{EW}$  can be represented by the ‘‘projection’’ of  $\vec{\Phi}$  onto  $\mathcal{H}$  being nonzero after applying a rotation onto  $\vec{F}$  (which was initially ‘‘perpendicular’’ to  $\mathcal{H}$  due to  $T^a \vec{F} = 0$ ), i.e.

$$v = f \sin \langle \theta \rangle \neq 0, \quad (3)$$

with  $f = |\vec{F}|$ .  $v$  is the VEV that causes the electroweak symmetry breaking. This is called the vacuum difference, i.e. the difference between the VEV of the  $\mathcal{G} \rightarrow \mathcal{H}$   $f$  breaking and the VEV of the electroweak symmetry breaking ( $v$ ). And unlike the technicolor model, the electroweak symmetry breaking in the CHM occurs if and only if the angle is very small,

$$\epsilon \equiv \frac{v^2}{f^2} = \sin^2 \langle \theta \rangle \ll 1. \quad (4)$$

Depending on how the model is constructed, the value of  $\epsilon$  can be obtained naturally, or it can be calibrated more or less.

To construct the CHM  $\mathcal{G} \rightarrow \mathcal{H}$ , where the electroweak group  $G_{EW} = SU(2) \times U(1) \subseteq \mathcal{H}$ , we need a complex Higgs doublet for it, i.e., at least 4 Goldstone bosons. To find the  $\mathcal{G}$  and  $\mathcal{H}$  groups, one way is to consider the breaking of  $SO(N)$  group. By the Goldstone’s theorem,

the spontaneous symmetry breaking  $SO(N) \rightarrow SO(N-1)$  will generate  $N-1$  Goldstone bosons. Thus, the smallest possible case of  $N$  is  $SO(5) \rightarrow SO(4)$ . The 10 generators of the group  $SO(5)$  in the basic representation,  $T^A = \{T^\alpha, \widehat{T}^{\hat{a}}\}$ , are divided into 2 parts as follows:

$$T^a = \left\{ T_L^\alpha = \begin{bmatrix} t_L^\alpha & \vec{0} \\ \vec{0}^T & 0 \end{bmatrix}, T_R^\alpha = \begin{bmatrix} t_R^\alpha & \vec{0} \\ \vec{0}^T & 0 \end{bmatrix} \right\} \quad (\alpha = 1, 2, 3), \quad (5)$$

$$(\widehat{T}^{\hat{a}})_{IJ} = -\frac{i}{\sqrt{2}}(\delta_I^i \delta_J^5 - \delta_J^i \delta_I^5). \quad (6)$$

The 6 generators  $T^a$  generate the group algebra  $SO(4)$  according to the generators of  $SU(2)_L \times SU(2)_R$  because  $SO(4)$  isomorphic to the chiral group  $SU(2)_L \times SU(2)_R$

$$\begin{aligned} (t_L^\alpha)_{ij} &= \frac{1}{4} \text{Tr} [\bar{\sigma}_i^\dagger \sigma^\alpha \bar{\sigma}_j] = -\frac{i}{2} [\varepsilon_{\alpha\beta\gamma} \delta_i^\beta \delta_j^\gamma + (\delta_i^\alpha \delta_j^4 - \delta_j^\alpha \delta_i^4)], \\ (t_R^\alpha)_{ij} &= \frac{1}{4} \text{Tr} [\bar{\sigma}_i \sigma^\alpha \bar{\sigma}_j^\dagger] = -\frac{i}{2} [\varepsilon_{\alpha\beta\gamma} \delta_i^\beta \delta_j^\gamma - (\delta_i^\alpha \delta_j^4 - \delta_j^\alpha \delta_i^4)]. \end{aligned} \quad (7)$$

We parameterize the 4 NGBs  $\Pi^{\hat{a}}$  corresponding to the 4 generators  $\widehat{T}^{\hat{a}}$  broken into

$$\vec{\Phi} = \exp \left[ i \frac{\sqrt{2}}{f} \Pi^{\hat{a}} \widehat{T}^{\hat{a}} \right] \vec{F} \equiv U[\vec{\Pi}] \vec{F}. \quad (8)$$

In which,  $U[\vec{\Pi}]$  is called the Goldstone matrix, which can be explicitly calculated as:

$$U[\vec{\Pi}] = \begin{bmatrix} I_4 - \left(1 - \cos \frac{|\Pi|}{f}\right) \frac{\vec{\Pi} \vec{\Pi}^T}{|\Pi|^2} & \sin \frac{|\Pi|}{f} \frac{\vec{\Pi}}{|\Pi|} \\ -\sin \frac{|\Pi|}{f} \frac{\vec{\Pi}^T}{|\Pi|} & \cos \frac{|\Pi|}{f} \end{bmatrix}, \quad (9)$$

where  $|\Pi| = \sqrt{\vec{\Pi}^T \vec{\Pi}}$ .

$$\vec{F} = \begin{bmatrix} \vec{0} \\ f \end{bmatrix} \Rightarrow \vec{\Phi} = f \begin{bmatrix} \sin \frac{|\Pi|}{f} \frac{\vec{\Pi}}{|\Pi|} \\ \cos \frac{|\Pi|}{f} \end{bmatrix}, \quad (10)$$

with  $f = |\vec{F}|$ . As said, 4  $\Pi^{\hat{a}}$  can form a 1/2 hypercharged Higgs bilinear:

$$\phi = \begin{bmatrix} \phi^+ \\ \phi^0 \end{bmatrix} = \frac{1}{\sqrt{2}} \begin{bmatrix} \Pi^2 + i\Pi^1 \\ \Pi^4 - i\Pi^3 \end{bmatrix} \Leftrightarrow \vec{\Pi} = \begin{bmatrix} \Pi^1 \\ \Pi^2 \\ \Pi^3 \\ \Pi^4 \end{bmatrix} = \frac{1}{\sqrt{2}} \begin{bmatrix} -i(\phi^+ - \phi^{+\dagger}) \\ \phi^+ + \phi^{+\dagger} \\ i(\phi^0 - \phi^{0\dagger}) \\ \phi^0 + \phi^{0\dagger} \end{bmatrix}. \quad (11)$$

This doublet  $\phi$  is the same one mentioned in the SM. And similar to the SM, we can choose the unitary gauge for  $\vec{\Pi}$

$$\phi = \begin{bmatrix} 0 \\ H \end{bmatrix} \text{ hay } \vec{\Pi} = \begin{bmatrix} 0 \\ 0 \\ H \\ 0 \end{bmatrix} \Rightarrow U[H] = \begin{bmatrix} I_3 & \vec{0} & \vec{0} \\ \vec{0}^T & c_H & s_H \\ \vec{0}^T & -s_H & c_H \end{bmatrix} \Rightarrow \vec{\Phi} = \begin{bmatrix} \vec{0} \\ f s_H \\ f c_H \end{bmatrix}, \quad (12)$$

with the field  $H$  considered in the perturbation of VEV  $\langle H \rangle = h$ , i.e.  $H(x) = h + \delta h(x)$  as in SM. The trigonometric functions have been re-noted for brevity:  $s_H \equiv \sin(H/f)$ ,  $c_H \equiv \cos(H/f)$ .

However, to be able to construct fermion multiplets in the MCHM, an additional group  $U(1)_X$  is needed, i.e.

$$SO(5) \otimes U(1)_X \rightarrow SO(4) \otimes U(1)_X. \quad (13)$$

We will embed the gauge field  $X_\mu$  of  $U(1)_X$  into the field  $B_\mu$  by setting  $X_\mu = B_\mu$  with the coupling constant also being  $g'$ . Then the hypercharge is redefined  $Y = T_R^3 + X$ . Each quark will have its own  $X$  to give the corresponding hypercharge.

To study the electroweak breaking in the MCHM, we need to write the effective lagrangian before the electroweak breaking. The Lagrangian includes the composite part in the near-vacuum state and the integration of resonance fields, the fields are not in the SM, out of the lagrangian. Specifically, we divide the Lagrangian into the following parts

$$\mathcal{L} = \mathcal{L}_\Phi + \mathcal{L}_g + \mathcal{L}_f - V_{\text{eff}}, \quad (14)$$

with the terms being the NGB part, the gauge boson part, the fermion part (top quark) and finally the effective potential energy. These components will be presented in the next section. We do not present the  $\mathcal{L}_g$  component, can refer to Ref.[53] because it is not related to the problem under consideration.

### A. Spectra of particles

The NGB part includes the kinetic energy of the NGB parametrized by the scalar field  $\vec{\Phi}$  mentioned earlier,

$$\mathcal{L}_\Phi = \frac{1}{2} D_\mu \vec{\Phi}^T D^\mu \vec{\Phi}, \quad (15)$$

with

$$D_\mu = \partial_\mu - igW_\mu^\alpha T_L^\alpha - ig'B_\mu T_R^3. \quad (16)$$

Here, if we consider  $\vec{\Pi}$  in the perturbation of VEV, the boson mass term is also derived similarly to SM,

$$\begin{aligned} D_\mu \vec{\Phi} &= \partial_\mu \vec{\Phi} - igW_\mu^\alpha T_L^\alpha \vec{\Phi} - ig'B_\mu T_R^3 \vec{\Phi} \\ &= \partial_\mu H \begin{bmatrix} \vec{0} \\ c_H \\ -s_H \end{bmatrix} - igW_\mu^\alpha \begin{bmatrix} t_L^\alpha & \vec{0} \\ \vec{0}^T & 0 \end{bmatrix} \begin{bmatrix} \vec{0} \\ fs_H \\ fc_H \end{bmatrix} - ig'B_\mu \begin{bmatrix} t_R^3 & \vec{0} \\ \vec{0}^T & 0 \end{bmatrix} \begin{bmatrix} \vec{0} \\ fs_H \\ fc_H \end{bmatrix} \\ &= \partial_\mu H \begin{bmatrix} \vec{0} \\ c_H \\ -s_H \end{bmatrix} - igf \sin \frac{H}{f} \left( -\frac{i}{2} \right) \begin{bmatrix} W_\mu^1 \\ W_\mu^2 \\ W_\mu^3 \\ 0 \\ 0 \end{bmatrix} - ig'B_\mu f \sin \frac{H}{f} \left( \frac{-i}{2} \right) \begin{bmatrix} 0 \\ 0 \\ -1 \\ 0 \\ 0 \end{bmatrix}. \quad (17) \end{aligned}$$

It will lead to

$$\begin{aligned} \frac{1}{2} |D_\mu \vec{\Phi}|^2 &= \frac{1}{2} |\partial_\mu H|^2 + \frac{f^2}{8} \sin^2 \frac{H}{f} [g^2 |W_\mu^1|^2 + g^2 |W_\mu^2|^2 + |gW_\mu^3 - g'B_\mu|^2] + \dots \\ &\approx \frac{1}{2} |\partial_\mu \delta h|^2 + \frac{f^2}{8} \sin^2 \frac{h}{f} [g^2 |W_\mu^+|^2 + g^2 |W_\mu^-|^2 + (g^2 + g'^2) |Z_\mu^0|^2] + \dots \quad (18) \end{aligned}$$

If  $\sin^2(h/f) = v/f$ , the masses of  $W^\pm$  and  $Z$  bosons are generated exactly as in SM. The mass functions of bosons are different from those in SM:

$$M_W^2 = \frac{g^2}{4} f^2 s_h^2, \quad M_Z^2 = \frac{g^2 + g'^2}{4} f^2 s_h^2. \quad (19)$$

Similar to SM, we consider only the contribution of top quark to be significant. In the UV, top quark interacts with the composite fields in the form of partial compositeness,

$$\mathcal{L}_f^{\text{UV}} = \mathcal{L}_f^{\text{kin}} + \sum_r \lambda_r \bar{\psi} \mathcal{O}_r + \text{h.c.} \quad (20)$$

The top and bottom quarks need to be embedded in  $\bar{\psi}$  with a suitable representation of SO(5) so that after breaking up they give the mass and interaction terms as SM. There are many ways to choose the representation for the multiplet and each will give different results.

The simplest is to use the **5** representation for each multiplet, namely

$$Q_L = \frac{1}{\sqrt{2}} \begin{bmatrix} -ib_L \\ -b_L \\ -it_L \\ t_L \\ 0 \end{bmatrix}, \quad T_R = \begin{bmatrix} 0 \\ 0 \\ 0 \\ 0 \\ t_R \end{bmatrix}. \quad (21)$$

In this case,  $t_L$  is embedded in the  $SO(4)$  quadruplet in the  $Q_L$  multiplet as above to be exactly equivalent to the  $\mathbf{2}_{-1/2}$  doublet. Note that the zero elements in the above multiplets are actually physical values of the non-dynamical fields, and since they have no physical role, we can safely set them to zero and continue the calculation. To be able to write the Lagrangian when the composite part is near the vacuum  $\vec{F}$ , we apply a Goldstone matrix to  $Q_L$  and  $T_R$ . We can do this because the quark multiplets have a global symmetry of  $SO(5)$  and the Goldstone matrix itself is a certain rotation of the  $SO(5)$  group,

$$Q_L \rightarrow U^{-1}Q_L \Rightarrow \bar{Q}_L \rightarrow \bar{Q}_L U = \frac{1}{\sqrt{2}} \bar{t}_L \begin{bmatrix} 0 & 0 & i & c_H & s_H \end{bmatrix}, \quad (22)$$

$$T_R \rightarrow U^{-1}T_R \Rightarrow \bar{T}_R \rightarrow \bar{T}_R U = \bar{t}_R \begin{bmatrix} 0 & 0 & 0 & -s_H & c_H \end{bmatrix}. \quad (23)$$

After the transformation, we can write the effective Lagrangian of the fermion part in the MCHM,

$$\begin{aligned} \mathcal{L}_{\text{mix}}^{\text{eff}} &= i\bar{q}_L \gamma^\mu D_\mu q_L + i\bar{t}_R \gamma^\mu D_\mu t_R \\ &+ \sum_{i=1}^{N_S} \bar{\psi}_1^i (i\gamma^\mu D_\mu - m_{1i}) \psi_1^i + \sum_{i=1}^{N_Q} \bar{\psi}_4^i (i\gamma^\mu D_\mu - m_{4i}) \psi_4^i \\ &+ \sum_{i=1}^{N_S} [y_{L1}^i f(\bar{Q}_L U)_1 \psi_1^i + y_{R1}^i f(\bar{T}_R U)_1 \psi_1^i + \text{h.c.}] \\ &+ \sum_{i=1}^{N_Q} [y_{L4}^i f(\bar{Q}_L U)_4 \psi_4^i + y_{R4}^i f(\bar{T}_R U)_4 \psi_4^i + \text{h.c.}]. \end{aligned} \quad (24)$$

In which,  $(\bar{Q}_L U)_{1,4}$  and  $(\bar{T}_R U)_{1,4}$  are the singlet and quadruplet in the pentaplet

$$\bar{Q}_L U \equiv [(\bar{Q}_L U)_4 \quad (\bar{Q}_L U)_1], \quad \bar{T}_R U \equiv [(\bar{T}_R U)_4 \quad (\bar{T}_R U)_1]. \quad (25)$$

$\psi_{1,4}$  are also the corresponding singlets and quadruplet generated by the  $\mathcal{O}$  operator. If we integrate the above Lagrangian out of the resonance fields, we get the effective Lagrangian of the top quark of the form

$$\mathcal{L}_f^{\text{eff}} = \bar{t}_L \not{p} \Pi_L(p^2) t_L + \bar{t}_R \not{p} \Pi_R(p^2) t_R - \bar{t}_L \Pi_{LR}(p^2) t_R - \bar{t}_R \Pi_{RL}(p^2) t_L. \quad (26)$$



In which

$$\begin{aligned}
\Pi_L(p^2) &= 1 - \frac{f^2}{2} s_H^2 \sum_{i=1}^{N_S} \frac{|y_{L1}^i|^2}{p^2 - m_{1i}^2} - \frac{f^2}{2} \sum_{i=1}^{N_Q} \frac{|y_{L4}^i|^2 + c_H^2 |y_{L4}^i|^2}{p^2 - m_{4i}^2} \\
&= 1 - f^2 \sum_{i=1}^{N_Q} \frac{|y_{L4}^i|^2}{p^2 - m_{4i}^2} + s_H^2 \frac{f^2}{2} \left[ - \sum_{i=1}^{N_S} \frac{|y_{L1}^i|^2}{p^2 - m_{1i}^2} + \sum_{i=1}^{N_Q} \frac{|y_{L4}^i|^2}{p^2 - m_{4i}^2} \right] \\
&\equiv \Pi_L^0(p^2) + s_h^2 \Pi_L^1(p^2),
\end{aligned} \tag{27}$$

$$\begin{aligned}
\Pi_R(p^2) &= 1 - f^2 c_H^2 \sum_{i=1}^{N_S} \frac{|y_{R1}^i|^2}{p^2 - m_{1i}^2} - f^2 s_H^2 \sum_{i=1}^{N_Q} \frac{|y_{R4}^i|^2}{p^2 - m_{4i}^2} \\
&= 1 - f^2 \sum_{i=1}^{N_S} \frac{|y_{R1}^i|^2}{p^2 - m_{1i}^2} + s_H^2 f^2 \left[ \sum_{i=1}^{N_S} \frac{|y_{R1}^i|^2}{p^2 - m_{1i}^2} - \sum_{i=1}^{N_Q} \frac{|y_{R4}^i|^2}{p^2 - m_{4i}^2} \right] \\
&\equiv \Pi_R^0(p^2) + s_H^2 \Pi_R^1(p^2),
\end{aligned} \tag{28}$$

$$\begin{aligned}
\Pi_{LR}(p^2) &= \frac{f^2}{\sqrt{2}} s_H c_H \sum_{i=1}^{N_S} y_{L1}^i y_{R1}^{i*} \frac{m_{1i}}{p^2 - m_{1i}^2} - \frac{f^2}{\sqrt{2}} s_H c_H \sum_{i=1}^{N_Q} y_{L4}^i y_{R4}^{i*} \frac{m_{4i}}{p^2 - m_{4i}^2} \\
&= \frac{f^2}{\sqrt{2}} s_H c_H \left[ \sum_{i=1}^{N_S} y_{L1}^i y_{R1}^{i*} \frac{m_{1i}}{p^2 - m_{1i}^2} - \sum_{i=1}^{N_Q} y_{L4}^i y_{R4}^{i*} \frac{m_{4i}}{p^2 - m_{4i}^2} \right] \\
&\equiv s_H c_H \Pi_{LR}^0(p^2),
\end{aligned} \tag{29}$$

$$\Pi_{RL}(p^2) = \Pi_{LR}^*(p^2) = s_H c_H \Pi_{LR}^{0*}(p^2) \equiv s_H c_H \Pi_{RL}^0(p^2). \tag{30}$$

The functions  $\Pi_{L,R}^{0,1}$  and  $\Pi_{LR,RL}^0$  need to return values that are true for the SM when considering the low-energy limit  $p^2 \approx 0$ . Specifically,

$$Z_{L,R} = \Pi_{L,R}^0(0) + \Pi_{L,R}^1(0)\epsilon, \tag{31}$$

$$m_t^2 = \frac{|\Pi_{LR}(0)|^2}{Z_L Z_R} = |\Pi_{LR}^0(0)|^2 \frac{\epsilon(1-\epsilon)}{Z_L Z_R} \approx \frac{|\Pi_{LR}^0(0)|^2}{\Pi_L^0(0)\Pi_R^0(0)} \epsilon(1-\epsilon). \tag{32}$$

Thus approximately, the mass of top quark has the form

$$M_t^2 = \frac{|\Pi_{LR}^0(0)|^2}{\Pi_L^0(0)\Pi_R^0(0)} s_h^2 c_h^2 = \frac{m_t^2}{\epsilon(1-\epsilon)} s_h^2 c_h^2 = \frac{y_t^2 f^2}{2(1-\epsilon)} s_h^2 c_h^2. \tag{33}$$

## B. The effective Higgs potential

The effective Higgs potential [54]

$$V_0(h) = \alpha^0 s_h^2 + \beta^0 s_h^4, \quad (s_h \equiv \sin(h/f), \quad c_h \equiv \cos(h/f)), \tag{34}$$

$$\begin{cases} \partial V/\partial h |_{h=\langle h \rangle} = 0 \\ \partial^2 V/\partial h^2 |_{h=\langle h \rangle} = m_h^2 \end{cases} \Rightarrow \begin{cases} \alpha^0 = -2\beta^0\epsilon \\ m_h^2 f^2 = 8\beta^0\epsilon(1-\epsilon) \end{cases}, \quad (35)$$

$$V_0(h) = \beta^0 (s_h^4 - 2\epsilon s_h^2) = \frac{m_h^2 f^2}{8\epsilon(1-\epsilon)} (s_h^4 - 2\epsilon s_h^2). \quad (36)$$

There are two things in the effective potential energy: (I) we need to achieve  $|\alpha^0| \ll |\beta^0|$  due to the condition  $\epsilon = -\alpha^0/2\beta^0 \ll 1$ ; (II)  $\beta^0 > 0$  for the mass term to be positive, which means  $\alpha^0 < 0$ . Depending on how the CHM is constructed, we can adjust  $\alpha^0$  and  $\beta^0$  so that the potential energy has the correct minimum and the Higgs mass is correct through the contributions of the additional resonances introduced. Whether the adjustment is large or not depends on the representation of fermion multiplets.

$$M_h^2 = \frac{m_h^2 f^2}{8\epsilon(1-\epsilon)} \frac{\partial^2 (s_h^4 - 2\epsilon s_h^2)}{\partial^2 h} = \frac{m_h^2}{2\epsilon(1-\epsilon)} (3s_h^2 - 4s_h^4 - \epsilon + 2\epsilon s_h^2). \quad (37)$$

The effective Higgs potential is of the form 34, we do not yet see the explicit contributions of other particles to this effective potential. Calculating their contributions is very complicated. The one-loop contributions of gauge, top quark, and Higgs fields **which comes from the resonance meson components**. There is a less dynamical alternative: We consider the particles as SM, and their contributions are calculated as SM, but now the masses of particles are functions of  $\sin(h/f)$ . Therefore, the effective potential at 0K and high temperature have the forms,

$$V_{\text{eff}}(h) = V_0(h) + \sum_{i=h,W,Z,t} \frac{n_i}{64\pi^2} \left[ M_i^4 \left( \log \frac{M_i^2}{m_i^2} - \frac{3}{2} \right) + 2M_i^2 m_i^2 \right]. \quad (38)$$

$$\begin{aligned} V_{\text{eff}}^\beta(h) &= V_{\text{eff}}(h) + \Delta V_1^\beta(h) \\ &= V_{\text{eff}}(h) + \sum_{i=h,W,Z} \frac{n_i}{2\pi\beta^4} J_B(\beta^2 M_i^2) - \frac{12}{2\pi\beta^4} J_F(\beta^2 M_t^2), \end{aligned} \quad (39)$$

in which

$$J_k(m^2\beta^2) = \int_0^\infty dx x^2 \ln \left[ 1 + n_k e^{-\sqrt{x^2 + \beta^2 m^2(\phi_c)}} \right], \quad \text{with } n_F = 1, n_B = -1. \quad (40)$$

The mass formulas of particles are functions that depend on  $s_h$ ,

$$\begin{aligned}
M_h^2 &= \frac{m_h^2 f^2}{8\epsilon(1-\epsilon)} \frac{\partial^2}{\partial h^2} (s_h^4 - 2\epsilon s_h^2) = \frac{m_h^2}{2\epsilon(1-\epsilon)} (3s_h^2 - 4s_h^4 - \epsilon + 2\epsilon s_h^2), \\
M_{W,Z}^2 &= \frac{m_{W,Z}^2}{\epsilon} s_h^2, \quad M_t^2 = \frac{m_t^2}{\epsilon(1-\epsilon)} (s_h^2 - s_h^4).
\end{aligned}
\tag{41}$$

Therefore, the meson resonance components are stored in the parameter  $\epsilon$ ,  $f$  and change the mass spectral formula of the particles compared to the SM.

Another way to sum all the contributions of SM particles is as in Ref.[55]. Also, in Refs. [51, 52, 54], the process of calculating the effective potential is similar to ours when the high temperature components are like the last two components in Eq.39. However, the authors consider the 0K components quite simply by including the contributions of the particles that are stored in the coefficients of the potential. This is also qualitatively reasonable, since the contributions of the particles at 0K do not have the trigger value for a first order phase transition. But to calculate the phase transition strength more accurately, we have done as above way with Eq.39.

### III. EWPT WITH THE CONFINEMENT SCALE OF THE STRONG SECTOR

With the effective potential Eq.39, we proceed to find the phase transition temperature  $T_c$  and the minimum  $h_m(T_c)$ . Then calculate the phase transition strength  $S = \frac{h_m(T_c)}{T_c}$ . The process can be solved numerically easily by running Eq.39 at different temperatures and finding their minima.

So we have a pre-chosen input parameter  $f$ , then run the effective potential with temperature and output the minimum value. The temperature and the minimum value that cancel the potential, are  $T_c$  and  $h_m(T_c)$  respectively. Since  $v = 246$  GeV, instead of choosing  $f$  we can choose  $\epsilon$ .

A first order phase transition is usually understood as  $S > 1$ . This comes from the decoupling condition [57] and analysis of the effective potential barrier (there exists a sufficiently large maximum between two minima such that the transition from zero to nonzero minimum is violent). This condition is essentially the most important condition in the Baryogenesis scenario. Hence, we expect an outcome  $S > 1$  in this model.

As mentioned earlier,  $\epsilon \lesssim 0.2$ , corresponding to  $f \gtrsim 550$  GeV, is of particular interest. Using the effective potential to probe the transition temperature at some values of  $f$  between

300 and 800 GeV (corresponding to  $\epsilon$  from 0.09 to 0.24), we get the results in Table I and Table II.

TABLE I: Phase transition intensity at  $f$  values from 500 to 800 GeV.

$f$ (GeV)	$\epsilon = v^2/f^2$	$T_c$ (GeV)	$h_m(T_c)$ (GeV)	$S = h_m(T_c)/T_c$
500	0.24	161.69	116.22	0.7187
530	0.22	160.59	107.21	0.6676
560	0.19	159.72	100.90	0.6317
590	0.17	159.03	95.50	0.6005
620	0.16	158.45	90.99	0.5742
650	0.14	157.98	87.39	0.5532
680	0.13	157.58	83.78	0.5317
710	0.12	157.23	81.08	0.5157
740	0.11	156.94	79.28	0.5052
770	0.10	156.68	77.48	0.4945
800	0.09	156.46	75.68	0.4837

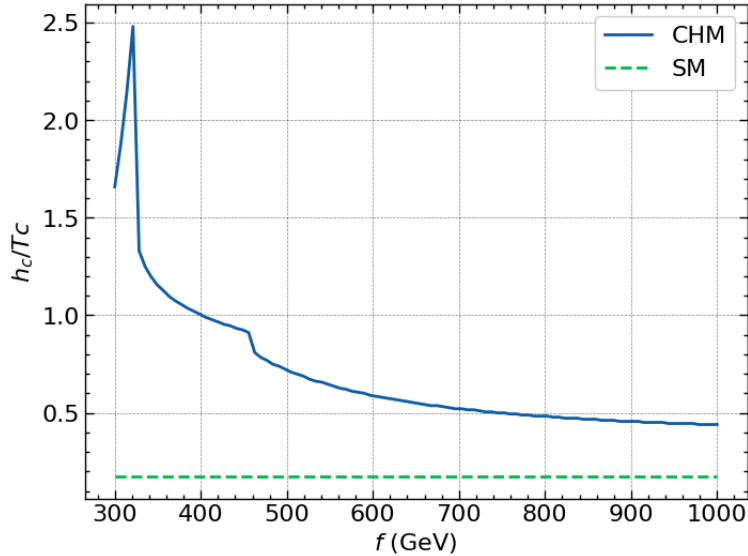


FIG. 1: Plot of phase transition intensity in CHM versus  $f$  (purple) and in SM (blue) in the range from 300 GeV to 1 TeV.

It can be clearly seen that the phase transition strength in this  $f$  region is larger than

TABLE II: Phase transition intensity at  $f$  values from 300 to 500 GeV.

$f$ (GeV)	$\epsilon = v^2/f^2$	$T_c$ (GeV)	$h_m(T_c)$ (GeV)	$S = h_m(T_c)/T_c$
300	0.67	284.30	471.17	1.6573
320	0.59	208.08	502.70	2.4159
340	0.52	181.52	220.72	1.2159
360	0.47	176.01	195.50	1.1107
380	0.42	172.16	180.18	1.0466
400	0.38	169.28	169.37	1.0005
420	0.34	167.03	161.26	0.9655
440	0.31	165.23	154.95	0.9378
460	0.29	163.72	134.23	0.8199
480	0.26	162.61	123.42	0.7590
500	0.24	161.69	116.22	0.7187

in the SM case and the phase transition strength increases as  $f$  decreases. Although this strength is still not enough to trigger a first order phase transition, the potential of CHM can still be seen since the composite part does indeed contribute to the phase transition strength. Indeed, it can be seen more clearly if we consider a larger  $f$  region, as long as  $f > v$ , at Figure 1. It can be seen from Fig.1 that the phase transition strength continues to increase as  $f$  decreases. Looking at the Table II, the phase transition strength has already surpassed 1 when  $f < 420$  GeV. The graph also breaks, with a sharp peak appearing in the  $f = 300 - 400$  GeV region. However, the behavior of the graph in the region  $\epsilon \approx 1$  is not really meaningful because the effective potential must satisfy  $s_h^2 \ll 1$ , and this approximation leads to some VEV Higgs region (not in the entire Higgs VEV one).

#### IV. EWPT WITH DILATON

From the results in the previous section, we can expect that the MCHM is not complete and there may be another way to explain and evaluate the phase transitions of MCHM. From the beginning of SecIII until now, we have assumed that the composite part breaks the symmetry before the electroweak symmetry breaking occurs. However, this is just an

assumption, because there is no reason why the symmetry of the composite part should be broken before the electroweak breaking. The Higgs-Dilaton Composite model is a model which built on the premise, the symmetries can be broken at the same time. Specifically, at high energies, the Lagrangian will contain an additional symmetry under the scale transformation  $x^\mu \rightarrow b^{-1}x^\mu$ . Then, this symmetry is broken at the same time as the electroweak breaking, and the breaking is described by the dilaton field  $\chi$ . The model is now no longer a tunneling of just the higgs minimum but of the common higgs-dilaton minimum.

### A. The Higgs-Dilaton potential in MCHM at 0K

There have been many analyses and numerical investigations of the dilaton potential and the interactions between the dilaton and the remaining fields in the model [51, 52, 54, 56]. Specifically, the dilaton field will cause the breaking of the scale symmetry when near VEV  $\chi$ . Since both the electroweak and scale symmetry are broken at the same time, the symmetry breaking occurs at the same momentum threshold  $m_*$ .

$$m_* = g_* f = g_\chi \chi. \quad (42)$$

Thus, in the effective potential,  $f$  now acts as a dynamic variable, not a constant as in the previous MCHM. To correct the Higgs potential to contain the Dilaton field, we can fix  $f$  to a value consistent with the old MCHM,  $f \approx 800$  GeV, corresponding to  $\chi_0 = g_* f / g_\chi$ . Then, the zero temperature potential of the Higgs is corrected by replacing the dynamic variable  $f$  with  $f\chi/\chi_0$  and  $f$  is fixed.

$$V_h(\chi, h) = \left(\frac{\chi}{\chi_0}\right)^4 V_0\left(\frac{h\chi_0}{\chi}\right) = \left(\frac{\chi}{\chi_0}\right)^4 \left(\alpha^0 \sin^2 \frac{h}{f\chi/\chi_0} + \beta^0 \sin^4 \frac{h}{f\chi/\chi_0}\right). \quad (43)$$

The factor  $(\chi/\chi_0)^4$  appears because  $\alpha^0$  and  $\beta^0$  are approximately proportional to  $f^4$ . Instead of leaving it as it is, we change the variable  $\hat{h} = h\chi_0/\chi$ . At the same time, the kinetic energy of the Higgs is corrected to

$$\frac{1}{2}(\partial_\mu \chi)^2 + \frac{1}{2}\left(\frac{\chi}{\chi_0}\right)^2 (\partial_\mu \hat{h})^2, \quad (44)$$

$g_\chi$  and  $g_*$  are the effective coupling constants from the large  $N$  approximation,

$$g_* = \frac{4\pi}{\sqrt{N}}, \quad g_\chi = \frac{4\pi}{\sqrt{N}}(\text{dilaton meson}) \quad \text{or} \quad g_\chi = \frac{4\pi}{N}(\text{dilaton glueball}). \quad (45)$$

In which,  $N$  is the color number in the gauge theory  $SU(N)$  at high energies, the dilaton meson will resemble the semi-composite interaction of the fermion part in the CHM, and the dilaton glueball will resemble the interaction of quarks in the technicolor model. Then,  $\chi_0$  also has two different values corresponding to the two cases above,

$$\chi_0 = \frac{g_* f}{g_\chi} = f \times \begin{cases} 1 & \text{for dilaton meson} \\ \sqrt{N}/2 & \text{for dilaton glueball} \end{cases}. \quad (46)$$

Furthermore, since the Yukawa constant (specifically that of Top quark) is also formed from the VEV of dilaton, this constant is also changed by the renormalization equation (RG), specifically the interaction between top quark and the composite part is changed,

$$\beta_\lambda(\chi) \equiv \frac{\partial \lambda_{t_{L,R}}}{\partial \ln \chi} = \gamma_\lambda \lambda_{t_{L,R}} + \frac{c_\lambda}{g_*^2} \lambda_{t_{L,R}}^3 \quad \left( y_t \approx \frac{\lambda_{t_L} \lambda_{t_R}}{g_*} \right). \quad (47)$$

By the NDA estimation method, the coefficients  $\alpha^0$  and  $\beta^0$  in the Higgs potential (with the  $\mathbf{5} \oplus \mathbf{5}$  representation of fermion) have the form

$$\alpha^{\text{NDA}} = c_\alpha \frac{N_c}{16\pi^2} \lambda_t^2 g_*^2 f^4, \quad \beta^{\text{NDA}} = c_\beta \frac{N_c}{16\pi^2} \lambda_t^4 f^4 \quad (\lambda_t = \max\{\lambda_{t_L}, \lambda_{t_R}\}). \quad (48)$$

This contradicts  $\alpha^0$  and  $\beta^0$  because  $\alpha^{\text{NDA}} \gg \beta^{\text{NDA}}$  ( $g_* \gg \lambda_t$ ) while we need  $\alpha^0 \ll \beta^0$ . This is a correction problem in MCHM. In fact, the least possible case that requires correction is the multiplet  $q_L$  in the  $\mathbf{14}$  representation of  $SO(5)$  and the singlet  $t_R$ . This representation still keeps the potential at  $V_0$ , but  $\alpha^{\text{NDA}}$  and  $\beta^{\text{NDA}}$  are now of the same size,

$$\alpha^{\text{NDA}} = c_\alpha \frac{N_c}{16\pi^2} \lambda_t^2 g_*^2 f^4, \quad \beta^{\text{NDA}} = c_\beta \frac{N_c}{16\pi^2} \lambda_t^2 g_*^2 f^4 \quad (\lambda_t = \lambda_{t_L}). \quad (49)$$

The correction required is now much smaller than the  $\mathbf{5} \oplus \mathbf{5}$  representation. We will use this result to correct the Higgs potential. Specifically, since  $\lambda_t$  varies with dilaton, we can correct by

$$\alpha^0 \longrightarrow \alpha^0 + \alpha^{\text{NDA}}(\chi) - \alpha^{\text{NDA}}(\chi_0), \quad (50)$$

$$\beta^0 \longrightarrow \beta^0 + \beta^{\text{NDA}}(\chi) - \beta^{\text{NDA}}(\chi_0). \quad (51)$$

Thus the full form of the Higgs potential at any dilaton  $\chi$  has the form

$$\begin{aligned} V_h(\chi, \hat{h}) &= \left( \frac{\chi}{\chi_0} \right)^4 \left( V_h^0(\hat{h}) + V_h^{\text{NDA}}(\chi, \hat{h}) \right). \\ V_h^0(\hat{h}) &= \alpha^0 s_h^2 + \beta^0 s_h^4 \\ V_h^{\text{NDA}}(\chi, \hat{h}) &= [\alpha^{\text{NDA}}(\chi) - \alpha^{\text{NDA}}(\chi_0)] s_h^2 + [\beta^{\text{NDA}}(\chi) - \beta^{\text{NDA}}(\chi_0)] s_h^4 \\ &= \frac{N_c}{16\pi^2} g_*^2 f^4 [\lambda_t^2(\chi) - \lambda_t^2(\chi_0)] (c_\alpha s_h^2 + c_\beta s_h^4). \end{aligned} \quad (52)$$

$\lambda_t^2(\chi)$  is calculated from the RG equation (47),

$$\ln \lambda_t - \frac{1}{2} \partial \ln \left( 1 + \frac{c_\lambda}{g_*^2} \lambda_t^2 \right) = \gamma_\lambda \partial \ln \chi, \quad (53)$$

$$\begin{aligned} \lambda_t^2(\chi) &= \frac{\gamma_\lambda}{\left( \frac{\chi_0}{\chi} \right)^{2\gamma_\lambda} \left[ \frac{\gamma_\lambda}{\lambda_t^2(\chi_0)} + \frac{c_\lambda}{g_*^2} \right] - \frac{c_\lambda}{g_*^2}} \\ &= \frac{(\chi/\chi_0)^{2\gamma_\lambda}}{1/\lambda_t^2(\chi_0) + c_\lambda/(g_*^2 \gamma_\lambda) [1 - (\chi/\chi_0)^{2\gamma_\lambda}]}, \end{aligned} \quad (54)$$

with  $\lambda_{tL}(\chi_0) \propto \sqrt{y_t g_*}$ . The Yukawa coupling of top quark  $y_t$  now also depends on  $\chi$  and is assumed to have the form,

$$y_t(\chi) = \frac{\lambda_{tL}}{g_*} [\lambda_{tR1}(\chi) + \lambda_{tR2}], \quad (55)$$

with  $\lambda_{tL}$  and  $\lambda_{tR2}$  being the initial parameters, and  $\lambda_{tR1}(\chi) \equiv \lambda_{tR}(\chi)$ .

## B. The Dilaton potential

Before considering the phase transition of the Higgs-dilaton potential, we need to determine the potential of dilaton itself. The dilaton potential is approximated at zero temperature as

$$V_\chi = c_\chi g_\chi^2 \chi^4 - \varepsilon(\chi) \chi^4, \quad (56)$$

with  $\varepsilon$  depending on the RG equation,

$$\beta_\varepsilon(\chi) \equiv \frac{\partial \varepsilon}{\partial \log \mu} = \gamma_\varepsilon \varepsilon + c_\varepsilon \frac{\varepsilon^2}{g_\chi^2}, \quad (57)$$

$c_\chi$  and  $c_\varepsilon$  are  $\mathcal{O}(1)$  coefficients, while  $\gamma_\varepsilon$  is assumed to be very small. The first term is the scale invariant, while the second term is responsible for breaking the scale symmetry depending on VEV  $\chi$ . Solving the above equation at  $\mu = g_\chi \chi$ , we find

$$\varepsilon(\chi) = \frac{(\chi/\chi_0)^{\gamma_\varepsilon}}{\frac{1}{\varepsilon_0} + \frac{c_\varepsilon}{\gamma_\varepsilon g_\chi^2} \left[ 1 - \left( \frac{\chi}{\chi_0} \right)^{\gamma_\varepsilon} \right]}. \quad (58)$$

$\gamma_\varepsilon$  and  $\varepsilon_0 \equiv \varepsilon(\chi_0)$  are determined by minimizing the potential at  $\chi = \chi_0$  and yielding the correct dilaton mass, a parameter is chosen initially. Minimizing  $V_\chi$ , we get

$$\varepsilon_0[\gamma_\varepsilon] = \frac{8c_\chi g_\chi^2}{(4 + \gamma_\varepsilon) + \sqrt{(4 + \gamma_\varepsilon)^2 + 16c_\chi c_\varepsilon}} \quad (59)$$



and  $\gamma_\epsilon$  is the solution of the equation

$$-\frac{m_\chi^2}{\chi_0^2} = 4(c_\chi g_\chi^2 - \epsilon_0[\gamma_\epsilon]) \left( \gamma_\epsilon + 4 + c_\epsilon \frac{2\epsilon_0[\gamma_\epsilon]}{g_\chi^2} \right), \quad (60)$$

with  $\epsilon_0 \equiv \epsilon(\chi_0)$ . The dilaton mass affects the depth of  $V_\chi$ . It can be seen from Figure 2 that the larger the dilaton mass is, the faster the dilaton potential decreases and the lower the minimum is.

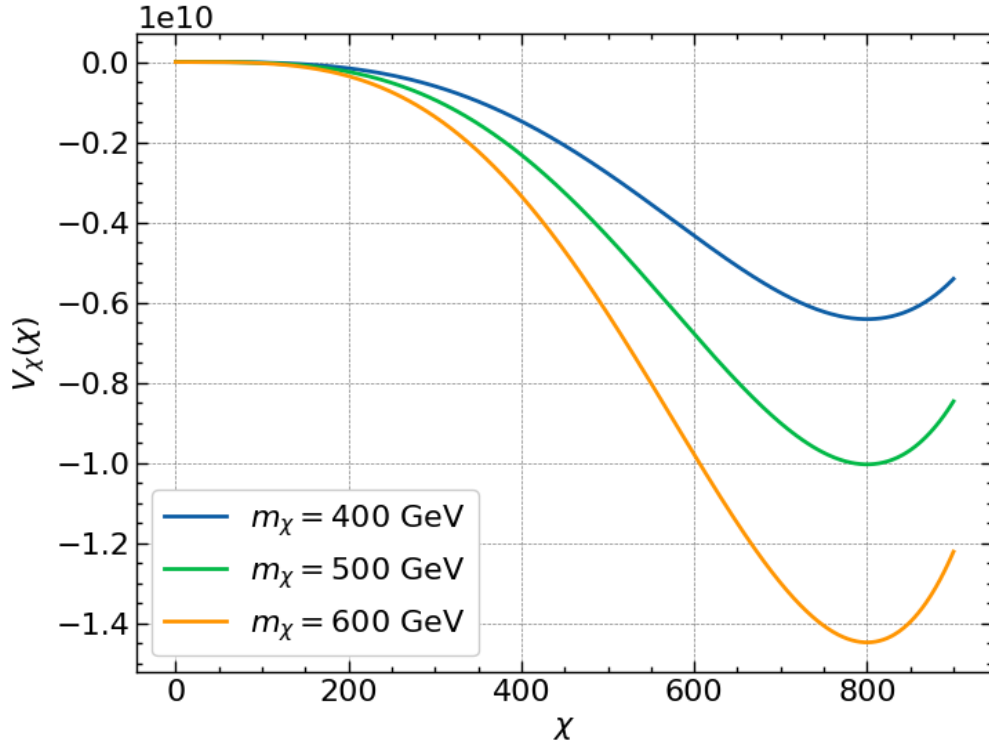


FIG. 2: The dilaton potential at the dilaton masses are 400 GeV, 500 GeV and 600 GeV (from top to bottom) respectively).

### C. The potential at high temperature

Having determined the dilaton's own potential and the higgs-dilaton potential, we can now move on to studying the potential at finite temperature. At  $\chi = 0$ , the normalized potential is

$$V_{\text{eff}}^\beta(0) = -\frac{\pi^2}{8} N^2 T^4 - \frac{\pi^2 g_{\text{SM}}}{90} T^4, \quad (61)$$

where,  $g_{\text{SM}} \approx 100$  is the total number of degrees of freedom of the entire SM. The first term is the value from the super Yang Mills theory  $\text{SU}(N)$  with  $\mathcal{N} = 4$ . When considering

the dilaton potential at finite temperature, the dilaton interval is divided into two regions: (I)  $0 \lesssim \chi \lesssim T/g_\chi$  and (II)  $\chi \gtrsim T/g_\chi$ . In region (II), the strong confinement scale  $g_\chi\chi$  is larger than the temperature under consideration, so the contribution of composite fields to the effective potential is very small. Therefore, the potential at a finite temperature also consists only of the corrected Higgs potential and the contributions of SM particles to the dilaton potential:

$$V_{\text{eff}}^\beta(\chi \gtrsim T/g_\chi, \hat{h}) = V_h + V_\chi + \Delta V_{\text{SM}}^\beta, \quad (62)$$

where  $\Delta V_{\text{SM}}$  are the temperature contributions of SM particles, including Higgs and dilaton, which are calculated by the  $J_{B,F}$  functions.

In region (I), the temperature is now higher than the strong confinement scale, so we need to know the full description in the ultraviolet limit to calculate the temperature-dependent corrections accurately.

Since the phase transition does not occur in this region either, the simplest way is to "connect" the potential at  $\chi = 0$  and region (II) by a step function.

Temporarily ignoring the Higgs-dependent terms and the contributions at finite temperature, we calculate the dilaton transition temperature by solving

$$V_{\text{eff}}^{1/T_c}(0) = V_{\text{eff}}^{1/T_c}(\chi_{\text{min}} \gtrsim T_c/g_\chi). \quad (63)$$

Also approximates the large  $N$  strongly interacting color limit to ignore the SM term in  $V_{\text{eff}}^\beta(0)$ ,

$$\begin{aligned} -\frac{\pi^2}{8}N^2T_c^4 \approx V_\chi(\chi_0) &= \left(1 - \frac{8}{4 + \gamma_\varepsilon + \sqrt{(4 + \gamma_\varepsilon)^2 - 16c_\varepsilon c_\chi}}\right) c_\chi g_\chi^2 \chi_0^4 \\ &\approx \left(1 - \frac{1}{1 + \gamma_\varepsilon/4}\right) c_\chi g_\chi^2 \chi_0^4 \approx \frac{\gamma_\varepsilon}{4} c_\chi g_\chi^2 \chi_0^4 = \frac{\gamma_\varepsilon}{4} \frac{g_*^4}{g_\chi^2} c_\chi f^4. \end{aligned} \quad (64)$$

Thus the phase transition temperature can be estimated as

$$T_c \approx \frac{g_* f}{\sqrt{\pi N} g_\chi} (-2\gamma_\varepsilon c_\chi)^{1/4} = 2f(-2\gamma_\varepsilon c_\chi)^{1/4} \times \begin{cases} N^{-3/4} & \text{for dilaton meson,} \\ (2N)^{-1/2} & \text{for dilaton glueball.} \end{cases} \quad (65)$$

This means that the phase transition strength increases with increasing  $N$ . Furthermore, considering the components that we have approximately neglected would deepen the potential at the minimum and thus reduce the transition temperature.

However, instead of using a step function, it is more convenient to adjust the effective potential to be a smooth and continuous function over region (I). We will enter a term in the effective potential in region (II) that is the one loop temperature contribution of the CFTs,  $\Delta V_\chi^\beta(\chi)$ ,

$$V_{\text{eff}}(\chi) = V_h + V_\chi + \Delta V_{\text{SM}}^\beta + \Delta V_\chi^\beta, \quad (66)$$

with

$$\Delta V_\chi^\beta(\chi) = \sum_{\text{CFT boson}} \frac{n_B J_B(\beta^2 g_\chi^2 \chi^2)}{2\pi^2 \beta^4} - \sum_{\text{CFT fermion}} \frac{n_F J_F(\beta^2 g_\chi^2 \chi^2)}{2\pi^2 \beta^4}. \quad (67)$$

Since the above two contributions are not much different, we can assume that only the fermion resonance contribution is zero and

$$\sum_{\text{boson resonance}} n = \frac{45N^2}{4} \quad (68)$$

so that  $\Delta V_{\text{eff}}^\beta(\chi, \hat{h})$  returns the same value in the super Yang-Mills model as in the remaining domain.

#### D. The numerical results

TABLE III: Parameters involved in solving the Higgs-Dilaton EWPT.

$c_\varepsilon$	$c_\chi$	$c_\alpha$	$c_\beta$	$\gamma_\lambda$	$c_\lambda$	$\lambda_{t_R}(\chi_0)$
0.5	0.2	-0.3	0.3	-0.3	1.875	$0.6\sqrt{y_t g_*}$

We conduct the EWPT survey as follows:

- **Step 1:** Choose the parameters as in the Table III (in Ref. [51]),  $f = 800$  GeV. Considering the case where the dilaton is a meson, we can deduce that  $\chi_0 = 800$  GeV. Determine  $\lambda_t(\chi)$  through the RG equation (47).
- **Step 2:** Choose a value of  $m_\chi$  to find  $\varepsilon(\chi)$  by solving the system of differential equations:

$$\begin{cases} \text{The RG Equation (57)} \\ V'_\chi(\chi_0) = 0 \\ V''_\chi(\chi_0) = m_\chi^2 \end{cases} \quad (69)$$

This gives the specific form of the dilaton potential (56). For the larger  $m_\chi$  is, the larger  $\varepsilon$  becomes in the range  $\chi$  from 0 to  $\chi_0$  (Figure 3).

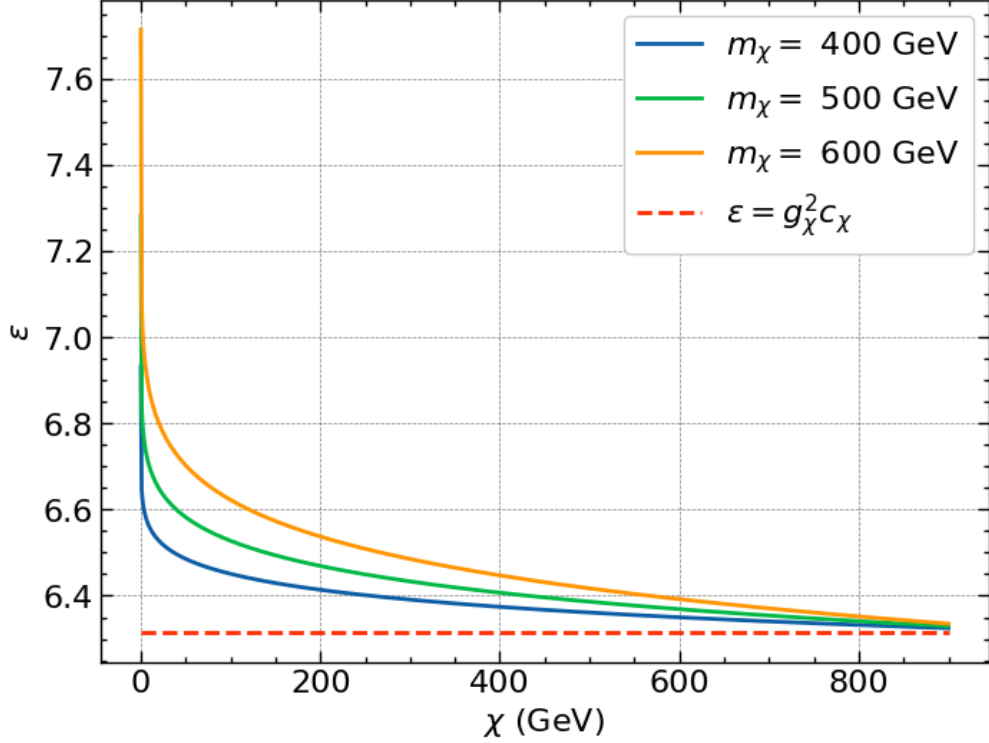


FIG. 3:  $\varepsilon(\chi)$  with different dilaton masses.

• **Step 3:** Determine the remaining potential terms in the total potential

- The potential  $V_h$  according to the equation (52).
- The one loop contributions according to the Coleman-Weinberg formula with mass functions recalibrated to contain  $\chi$

$$M_{W,Z}^2(\chi, \hat{h}) = \left(\frac{\chi}{\chi_0}\right)^2 M_{W,Z}^2(\hat{h}) = \left(\frac{\chi}{\chi_0}\right)^2 \frac{m_{W,Z}^2}{\varepsilon} \sin^2 \frac{\hat{h}}{f}. \quad (70)$$

$$M_t^2(\chi, \hat{h}) = \left(\frac{\chi}{\chi_0}\right)^2 \frac{y_t^2(\chi)}{2} f^2 \sin^2 \frac{\hat{h}}{f}. \quad (71)$$

$$M_h^2(\chi, \hat{h}) = \left(\frac{\chi}{\chi_0}\right)^2 \frac{1}{f^2} [2\alpha(\chi)(c_h^2 - s_h^2) + \beta(\chi)(12s_h^2 c_h^2 - 4s_h^4)]. \quad (72)$$

- The one loop contributions using Coleman-Weinberg formula after renormalization

$$\Delta V_h^1(\chi, \hat{h}) = \left(\frac{\chi}{\chi_0}\right)^4 \sum_{i=h,W,Z,t} \left[ M_i^4 \left( \log \frac{M_i^2}{m^2} - \frac{3}{2} \right) + 2M_i^2 m_i^2 \right], \quad (73)$$

with  $m_i = M_i(\chi, \langle h \rangle)$

- The one loop contributions of h, W,B, t at temperatures, to the higgs potential by the temperature functions  $J_B$  and  $J_F$

$$\Delta V_{\text{SM}}^T(T, \chi, \hat{h}) = \sum_{i=h,W,Z} \frac{n_i T^4}{2\pi^2} J_B\left(\frac{M_i^2}{T^2}\right) - \frac{12T^4}{2\pi^2} J_F\left(\frac{M_t^2}{T^2}\right). \quad (74)$$

And the total potential is

$$V_{\text{eff}}(T, \chi, \hat{h}) = V_\chi(\chi) + V_h(\chi, \hat{h}) + \Delta V_h^1(\chi, \hat{h}) + \Delta V_{\text{SM}}^T(T, \chi, \hat{h}). \quad (75)$$

Note that the total potential needs to be normalized so that  $V_{\text{eff}}(T, 0, 0) = 0$

- **Step 4:** Find the critical temperature  $T_c$  and  $(\chi_c, \hat{h}_c)$  which are the minima of  $V_{\text{eff}}(T_c, \chi_c, \hat{h}_c)$  such that

$$V_{\text{eff}}(T_c, \chi_c, \hat{h}_c) = -\frac{\pi^2 N^2}{8} T_c^4 - \frac{\pi^2 g_{\text{SM}}}{90} T_c^4, \quad (76)$$

or

$$V_{\text{eff}}(T_c, \chi_c, \hat{h}_c) + \frac{\pi^2 N^2}{8} T_c^4 + \frac{\pi^2 g_{\text{SM}}}{90} T_c^4 = 0. \quad (77)$$

Then  $T_c$  is the phase transition temperature. Fixing the CFT color number  $N = 5$  and  $g_{\text{SM}} = 100$ .

The above steps are performed with  $m_\chi$  in the mass range from 300 to 800 GeV. The results give four graphs corresponding to  $\chi_c$ ,  $h_c$ ,  $T_c$  and  $h_c/T_c$  against the dilaton mass  $m_\chi$  at Figure 4 and the corresponding data at Table IV. It can be seen from the graphs that the dilaton mass clearly affects the minimum state of the model. As the dilaton mass increases,  $\chi_c$  also increases and gets closer and closer to  $\chi_0$ . This shows that the larger the dilaton mass is, the less the minimum of the total potential energy is affected by the higgs potential, leading to  $\chi_0$  also being almost the minimum of the total potential. This is also reasonable because the minimum of dilaton potential becomes deeper and narrower. Also, the required transition temperature increases with the depth of the minimum, and as the temperature increases, the Higgs potential minimum becomes increasingly smaller due to the contribution at a finite temperature.

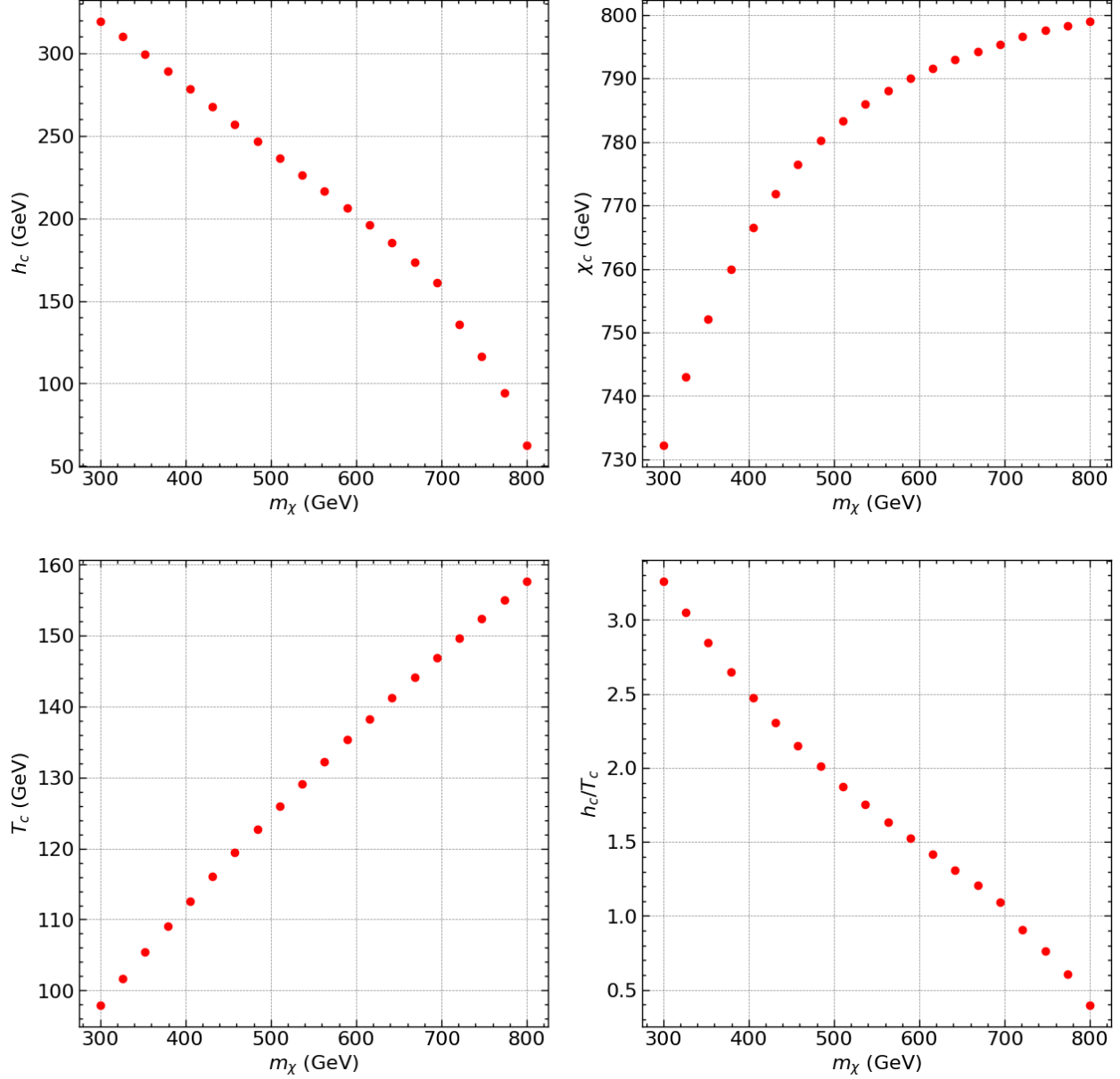


FIG. 4: Phase transitions with dilaton masses in the range from 300 GeV to 800 GeV.

Considering the possibility of first order transition, the overall transition strength in the Higgs-dilaton model is larger than in both the SM and CHM in the range of  $m_\chi$  considered. The transition strength can be larger than 1 when  $m_\chi < 700$  GeV. Furthermore, the minimum of dilaton potential lies in the vicinity of  $\chi_0$ , while  $f$  in the CHM is only below 400 GeV for  $h_c/T_c > 1$ . This shows that the dilaton not only helps to trigger the first order EWPT but also helps this process to occur in a suitable value range, without breaking the approximation of  $\sin^2(h/f)$ .

TABLE IV: Phase transitions at  $f = 800$  GeV and  $m_\chi$  from 300 GeV to 800 GeV.

$m_\chi$ (GeV)	$T_c$ (GeV)	$h_c(T_c)$ (GeV)	$\chi_c(T_c)$ (GeV)	$S = h_c(T_c)/T_c$
300.00	97.92	732.21	319.43	3.2623
326.32	101.67	742.92	309.84	3.0475
352.63	105.37	752.12	299.56	2.8430
378.95	109.00	759.92	288.91	2.6506
405.26	112.55	766.45	278.15	2.4713
431.58	116.03	771.89	267.45	2.3051
457.89	119.42	776.41	256.91	2.1513
484.21	122.74	780.17	246.56	2.0087
510.53	125.99	783.30	236.38	1.8762
536.84	129.16	785.93	226.31	1.7521
563.16	132.27	788.14	216.26	1.6350
589.47	135.31	790.01	206.14	1.5235
615.79	138.29	791.62	195.80	1.4158
642.11	141.22	793.00	185.06	1.3104
668.42	144.09	794.21	173.62	1.2050
694.74	146.90	795.30	160.87	1.0950
721.05	149.67	796.65	135.70	0.9066
747.37	152.40	797.54	116.48	0.7643
773.68	155.08	798.32	94.44	0.6090
800.00	157.72	799.05	62.62	0.3970

## V. CONCLUSION AND OUTLOOKS

The paper shows that the Minimal Composite Higgs Model has a stronger electroweak transition strength than the Standard Model. The SM is most likely an effective theory and the effect of the composite components changes the shape of the potential, leading to a change in the electroweak transition.

The MCHM alone is not sufficient to trigger an electroweak transition compatible with the

conditions of  $f$ . When  $f$  is varied in the range 300 – 800 GeV the model suggests that with a confinement scale  $f$  smaller than a suitable value, the transition strength can be achieved. This leads to the possibility that  $f$  is a dynamical field and the electroweak transition occurs before  $f$  reaches its vacuum value. The fixed confinement scale  $f$  is then upgraded to a dilaton dynamical field  $\chi$ . By modifying the Composite Higgs model to include the dilaton appropriately, the barrier between the two vacuums is significantly increased, leading to a naturally large phase transition strength of 1 and the electroweak phase transition still occurring in the dilaton region consistent with the approximations in the Composite Higgs model. At zero temperature, the dilaton potential and the Higgs potential remain independent of each other. However, at finite temperatures the Higgs and dilaton interact with each other through the presence of dilaton in the Higgs potential, thereby triggering the first order EWPT.

Physically, the presence of dilaton may be an important contribution of the composite part that we may have overlooked when making the approximations in the MCHM. This occurs in the CHM due to the complexity of translating high-energy interactions to low-energy ones (the  $\Pi$  functions in the interaction of top quark and the resonance fields) and the lack of understanding of physics at a very high energies to be able to give the correct form of the Lagrangian as well as the effective potential.

The study of the Higgs-Dilaton model in the paper has shown the potential of dilaton in satisfying the thermodynamic condition of one of the three Sakharov conditions, however, this model still has many unknown parameters, because the knowledge of physics at very high energies is still limited. Therefore, the results require investigation with many different sets of parameters. In addition, because the dilaton increases the complexity of potential as well as the number of variables of the system, the calculation needs to be done numerically and requires a lot of resources to be able to investigate with a large number of different parameter cases.

With the introduction of dilatons, further studies on the effects of dilaton on the interaction constants and experimentally tested parameters can be conducted to constrain the possible parameters. In addition, the results can be further constrained by further studies on the effects of dilatons on the remaining conditions for baryogenesis from electroweak phase transitions.



## ACKNOWLEDGMENTS

This research is funded by Vietnam National Foundation for Science and Technology Development (NAFOSTED) under grant number 103.01-2023.16.

---

- [1] A. D. Sakharov, *JETP Lett.* **5**, 24 (1967).
- [2] Vo Quoc Phong, Vo Thanh Van, and Hoang Ngoc Long, *Phys. Rev. D* **88**, 096009 (2013).
- [3] A. Menon, D. E. Morrissey, and C. E. M. Wagner, *Phys. Rev. D* **70**, 035005 (2004).
- [4] S. W. Ham, S. K. Oh, C. M. Kim, E. J. Yoo, and D. Son, *Phys. Rev. D* **70**, 075001 (2004).
- [5] M. Bastero-Gil, C. Hugonie, S. F. King, D. P. Roy, and S. Vempati, *Phys. Lett. B* **489**, 359 (2000).
- [6] A. Menon, D. E. Morrissey, and C. E. M. Wagner, *Phys. Rev. D* **70**, 035005 (2004).
- [7] J. M. Cline, G. Laporte, H. Yamashita, S. Kraml, *JHEP* **0907**, 040 (2009).
- [8] A. Azatov, M. Vanvlasselaer, *JHEP* **09**, 085 (2020).
- [9] G. C. Dorsch, S. J. Huber, J. M. No, *JHEP* **10**, 029 (2013).
- [10] S. W. Ham, S-A Shim, and S. K. Oh, *Phys. Rev. D* **81**, 055015 (2010).
- [11] D. Borah and J. M. Cline, *Phys. Rev. D* **86**, 055001 (2013).
- [12] A. Ahriche and S. Nasri, *Phys. Rev. D* **85**, 093007 (2012).
- [13] S. Das, P. J. Fox, A. Kumar, and N. Weiner, *JHEP* **1011**, 108 (2010).
- [14] D. Chung and A. J. Long, *Phys. Rev. D* **84**, 103513 (2011).
- [15] M. Carena, N. R. Shaha, and C. E. M. Wagner, *Phys. Rev. D* **85**, 036003 (2012).
- [16] V. Q. Phong, H. N. Long, V. T. Van, N. C. Thanh, *Phys. Rev. D* **90**, 085019 (2014).
- [17] J. Sá Borges, R. O.Ramos, *Eur. Phys. J. C* **76**, 344 (2016).
- [18] V. Q. Phong, H. N. Long, V. T. Van, L. H. Minh, *Eur. Phys. J. C* **75**, 342 (2015).
- [19] J. R. Espinosa, T. Konstandin and F. Riva, *Nucl. Phys. B* **854**, 592 (2012).
- [20] D. J. H. Chung and A. J. Long, *Phys. Rev. D* **81**, 123531 (2010).
- [21] G. Barenboim and N. Rius, *Phys. Rev. D* **58**, 065010 (1998).
- [22] S. Profumo, M. J. Ramsey-Musolf, G. Shaughnessy, *JHEP* **0708**, 010 (2007).
- [23] S. Profumo, M. J. Ramsey-Musolf, C. L. Wainwright, P. Winslow, *Phys. Rev. D* **91**, 035018 (2015).

- [24] D. Curtin, P. Meade, C-T. Yu, JHEP **11**, 127 (2014).
- [25] M. Jiang, L. Bian, W. Huang, J. Shu, Phys. Rev. D **93**, 065032 (2016).
- [26] M. Carena, G. Nardini, M. Quiros, C. E.M. Wagner, Nucl. Phys. B **812**, 243-263 (2009).
- [27] A. Katz, M. Perelstein, M. J. Ramsey-Musolf, P. Winslow, Phys. Rev. D **92**, 095019 (2015).
- [28] J. Kozaczuk, S. Profumo, L. S. Haskins, C. L. Wainwright, JHEP **1501**, 144 (2015).
- [29] H. H. Patel, M. J. Ramsey-Musolf, Phys.Rev. D. **88**, 035013 (2012).
- [30] N. Blinov, J. Kozaczuk, D. E. Morrissey, C. Tamarit, Phys. Rev. D **92**, 035012 (2015).
- [31] S. Inoue, G. Ovanessian, M. J. Ramsey-Musolf, Phys. Rev. D **93**, 015013 (2016).
- [32] H. H. Patel, M. J. Ramsey-Musolf, JHEP **1107**, 029 (2011).
- [33] G. W. Anderson and L. J. Hall, Phys. Rev. D **45**, 2685 (1992).
- [34] H. H. Patel and M.J. Ramsey-Musolf, M. Garny and T. Konstandin, JHEP **1207**, 189 (2012).
- [35] J. De Vries, M. Postma, J. van de Vis, JHEP **1904**, 024 (2019).
- [36] J. de Vries, M. Postma, J. van de Vis , G. White, JHEP **1801**, 089 (2018).
- [37] C. Balazs, G. White, J. Yue, JHEP **1703**, 030 (2017).
- [38] A. Ahriche, Phys. Rev. D **75**, 083522 (2007).
- [39] A. Ahriche, Eur. Phys. J. C **66**, 333 (2010).
- [40] T. A. Chowdhury and S. Nasri, JHEP **1411**, 096 (2014).
- [41] A. Ahriche and S. Nasri, JCAP **1307**, 035 (2013).
- [42] M. Spannowsky and C. Tamarit, Phys. Rev. D **95**, 015006 (2017).
- [43] C. Grojean, G. Servant, J. D. Wells, Phys. Rev. D **71** 036001 (2005).
- [44] C. Delaunay, C. Grojean, J. D. Wells, JHEP **0804**, 029 (2008).
- [45] A. Kusenko, L. Pearce, and L. Yang, Phys. Rev. Lett. **114**, 061302 (2015).
- [46] Vo Quoc Phong, N. T. Tuong, N. C. Thao, H. N. Long, Phys. Rev. D **99**, 015035 (2019).
- [47] A. Braconi, Mu-Chun Chen, G. Gaswint, Phys. Rev. D **100**, 015032 (2019).
- [48] I. Baldes, T. Konstandin, G. Servant, Phys. Lett. B **786**, 373 (2015).
- [49] M. J. Dugan, H. Georgi, and D. B. Kaplan, Nuclear Physics B **254**, 299 (1985).
- [50] K. Fujikura, Y. Nakai, R. Sato, and Y. Wang, JHEP **09**, 053 (2023).
- [51] S. Bruggisser, B. Von Harling, O. Matsedonskyi, and G. Servant, Phys. Rev. Lett. **121**, 131801 (2018).
- [52] S. Bruggisser, B. Von Harling, O. Matsedonskyi, and G. Servant, JHEP **1812** , 099 (2018).
- [53] K. Agashe, R. Contino, and A. Pomarol, Nuclear Physics B, vol. 719, pp. 165–187, July 2005.

- [54] S. Bruggisser, B. Von Harling, O. Matsedonskyi, and G. Servant, *JHEP* **08**, 012 (2023).
- [55] Ben Gripaios,<sup>a</sup> Alex Pomarol,<sup>b</sup> Francesco Riva,<sup>a,c</sup> and Javi Serrab, *JHEP* **04**, 070 (2009).
- [56] B. Von Harling, O. Matsedonskyi, and G. Servant, *JHEP* **12**, 138 (2023).
- [57] P. Arnold and L. D. McLerran, *Phys. Rev. D* **36**, 581 (1987).